An adaptive grid refinement method for the relativistic Vlasov-Maxwell equations

N. Elkina

Ludwig-Maximilians University, München, Germany

Despite the obvious limitations associated with high dimension the grid based Vlasov-Maxwell numerical solution of the following system

$$\frac{\partial f_\alpha}{\partial t}+\frac{u}{\gamma}\frac{\partial f_\alpha}{\partial x}+\frac{e_\alpha}{m_\alpha}\left(\vec{E}+\frac{\vec{u}\times\vec{B}}{\gamma c}\right)\frac{\partial f_\alpha}{\partial \vec{u}}=0 \tag{1}$$

$$\frac{1}{c}\frac{\partial \vec{E}}{\partial t}=\nabla\times\vec{B}-\frac{4\pi}{c}\vec{J},\quad -\frac{1}{c}\frac{\partial \vec{B}}{\partial t}=\nabla\times\vec{E}, \tag{2}$$

$$\rho=\sum_\alpha e_\alpha\int f_\alpha d\vec{u},\quad \vec{J}=\sum_\alpha e_\alpha\int\frac{\vec{u}}{\gamma}f_\alpha d\vec{u}. \tag{3}$$

constantly attract attention in both space and laboratory plasmas communities. The idea to relive the computational complexity by utilizing an Adaptive Mesh Refinement (AMR) comes up naturally. The example of adaptive mesh is shown in Figure 1. In this paper we present adaptive electromagnetic Vlasov-Maxwell solver dealing with a special class of distribution functions

$$f(x,\,\vec{u})=f(x,\,u_x)\delta\left(\vec{u}_\perp+(e/m)\vec{A}_\perp\right). \tag{4}$$

Although its simplicity this distribution function allows describe relativistic in laser driven plasma. and quickly test various numerical techniques with modest computational resources. In the following we apply finite volume technique to the Vlasov equations due to its well-recognized advantage to deal with any kind of mesh without degrading the conservation property. The finite volume method applied in our code requires the Vlasov-Maxwell equations to be recast in a conservative form. For (4) the Vlasov equation reduces to

$$\frac{\partial f}{\partial t}+\nabla\cdot(\vec{\Psi}f)=0,\quad \vec{\Psi}=\frac{d\vec{R}}{dt}=\left(\frac{u_x}{\gamma},\,\frac{e}{m}E_x-\frac{1}{2\gamma}\frac{\partial a_\perp^2}{\partial x}\right) \tag{5}$$

Generic semi-discrete finite volume scheme reads with fluxes $(f\vec{\Psi})\to\{F,\,G\}$

$$\frac{d\overline{q}_{i,j}}{dt}=-\frac{F_{i+1/2,\,j}-F_{i-1/2,\,j}}{\Delta^x_{i,j}}-\frac{G_{i,\,j+1/2}-G_{i,\,j-1/2}}{\Delta^y_{i,j}} \tag{6}$$

admits central-upwind flux approximation [1] where flux

$$F_{i+1/2,j}=\frac{a^x}{2}\left[f(q^-_{i+1/2,j})+f(u^+_{i+1/2,j})\right]-\frac{a^x}{2}\left(q^+_{i+1/2,j}-q^-_{i+1/2,j}\right), \tag{7}$$

where a^x is the local speeds of solution propagation estimate as $a^x = \max(\lambda_k(\partial_{\vec{q}}\vec{F}(\vec{q})),\, 0) = c$. The flux $F(q^+_{i+1/2}, q^{i-1/2}_{i+1/2})$ have to be supplemented with an appropriate reconstruction of pointwise values of the solution at the cell edges. Here we consider a piece-wise linear reconstruction

$$q_{i,j}(x,y) = \overline{q}_{i,j} + D^x_{i,j}\cdot(x - x_i) + D^y_{i,j}\cdot(y - y_j), \tag{8}$$

$$D^x_{i,j} = \frac{\overline{q}_{i+1,j} - \overline{q}_{i-1,j}}{2\Delta x}, \quad D^y_{i,j} = \frac{\overline{q}_{i,j+1} - \overline{q}_{i,j-1}}{2\Delta x} \tag{9}$$

The piece-wise linear reconstruction on is not guarded to be monotone in the presence of discontinuities. Monotonicity imply that the cell average remains bounded by the values of neighbors including corner ones, i.e. $\min(\mathbf{Q}_{i,j}) < q_{i,j}(x,y) < \max(\mathbf{Q}_{i,j})$. The matrix $\mathbf{Q}_{ij}$ is formed by immediate neighbors of the cell (i,j). The slope-limiting procedure can be summarized as follows. First, we calculate matrix of slopes

$$\mathbf{D}^{\pm}_x = \begin{bmatrix} (\overline{q}_{i-1,j+1} - \overline{q}_{i,j}) & (\overline{q}_{i,j+1} - \overline{q}_{i,j}) & (\overline{q}_{i+1,j+1} - \overline{q}_{i,j}) \\ (\overline{q}_{i-1,j} - \overline{q}_{i,j}) & \pm\varepsilon & (\overline{q}_{i+1,j} - \overline{q}_{i+1,j}) \\ (\overline{q}_{i-1,j-1} - \overline{q}_{i,j}) & (\overline{q}_{i,j-1} - \overline{q}_{i,j-1}) & (\overline{q}_{i+1,j-1} - \overline{q}_{i+1,j}) \end{bmatrix} \tag{10}$$

Here the constant $\varepsilon = 10^{-20}$ was introduced to ensure continuous dependence on the data. The new slopes for (9) are defined as

$$D^x_{i,j} = \min(w^{pp}, w^{pm}, w^{mp}, w^{mm}) \cdot \left[\overline{q}_{i+1,j} - \overline{q}_{i-1,j}\right]/2, \tag{11}$$

$$D^y_{i,j} = \min(w^{pp}, w^{pm}, w^{mp}, w^{mm}) \cdot \left[\overline{q}_{i,j+1} - \overline{q}_{i,j-1}\right]/2. \tag{12}$$

where weights are calculated at corners. For upper-right corner w^{pp} we have

$$w^{pp} = \begin{cases} V_{\max}/u^{pp}, & u^{pp} > V_{\max}, \\ V_{\min}/u^{pp}, & u^{pp} < V_{\min}, \\ 1, & \text{otherwise} \end{cases}, \quad \text{where} \quad \begin{array}{l} V_{\min} = \min(\mathbf{D}^-) \\ V_{\max} = \max(\mathbf{D}^+). \end{array} \tag{13}$$

where u^{pp} is the reconstruction at upper-right corner, i.e. $u^{pp} = 0.5(D^x_{ij} + D^y_{ij})$. The scheme was extended to locally adaptive grid using conservative fluxes reconstruction. The algorithm can be summarized as follows; a newly created cell is initialized in a conservative manner using previous cell averages. The assigned cell average is computed by integration of the reconstruction polynomial over a newly created control volumes. We assume that the neighboring cell resolution is restricted by factor of two. In this case the

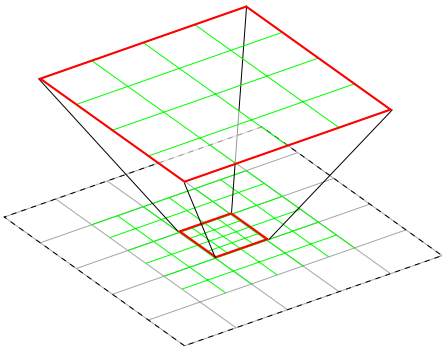

Figure 1: Adaptive mesh refinement

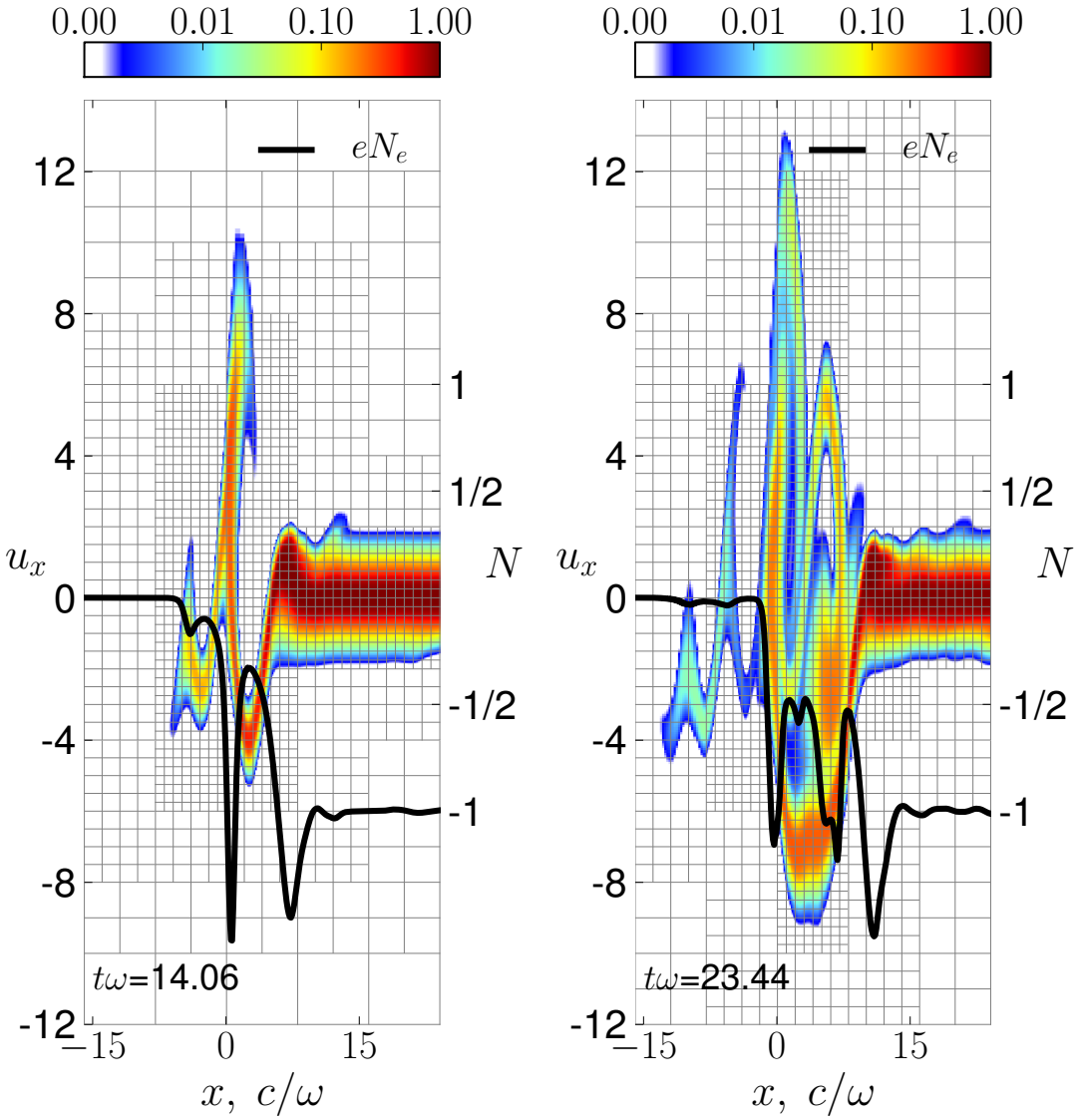

Figure 2: Electron distribution function in the course of laser plasma interaction.

communication between different levels of refinement maybe organized in form of boundary conditions provided by

$$q^l_{i,j} = \frac{4}{\Delta x \Delta y}\left[q^{l-1}_{ij}\frac{xy}{4} + D^{x,l-1}_{ij}\frac{x^2 y}{8} + D^{y,l-1}_{ij}\frac{y^2 x}{8}\right], \qquad (14)$$

$$q^l_{i,j} = \frac{1}{4}\left[q^{l+1}_{2i,2j} + q^{l+1}_{2i,2j+1} + q^{l+1}_{2i+1,2j} + q^{l+1}_{2i+1,2j+1}\right]. \qquad (15)$$

For detailed description of AMR procedure consult [2]. To demonstrate our code in action we perform simulation of a slab of plasma irradiated by a laser pulse [3]. Normally dense plasma is not transparent for electromagnetic radiation if $\omega_{pe} > \omega_0$, this condition defines a critical density $\omega_{pe}(n_{cr} = \omega_0)$, where $n_{cr} = \omega_0^2 m_e / 4\pi e^2$. If laser pulse becomes relativistic, i.e. $a_0 = eA/mc > 1$, then plasma frequency changes nonlinearly with the Lorenz factor $\omega_{pe} \sim \sqrt{1/\gamma}$ where $\gamma \sim a_0$. The initial condition for laser field is taken in form of circularly polarized laser pulse with the

Gaussian envelop

$$\vec{A}(t,x) = \frac{a_0}{\sqrt{2}} F(\varphi)\Big(\cos(\varphi)\vec{y} + \sin(\varphi)\vec{z}\Big). \tag{16}$$

where $\vec{A} = \{0,\ a_x,\ a_y\}$, $\varphi = \omega t - k_x x$. We consider a flat-top envelope $F(\varphi)$

$$F(\varphi) = \frac{1}{2}\Big(\tanh(\phi + \Delta_L) - \tanh(\varphi - \Delta_L)\Big), \tag{17}$$

where Δ_L is the chatacteristic width of the laser pulse. The plasma slab with initial density corresponding to $N = n_{cr}$ is initialize $0 < x < L_x$ where $L_x = 32\ c/\omega_0$ is the plasma slab width. The laser pulse width is $\Delta_L = 28c/\omega_0$, the laser frequency is $\omega = 1\ eV$. The plasma slab is initialized using the relativistic Maxwellian distribution function. The laser pulse is propagating from the left side of simulation box along x direction and collides with the plasma slab a $x = 0$. In the course of the interaction the radiation pressure of the incident laser pulse pushes the plasma electrons. That leads to building up a charge density gradient. As a result the longitudinal electric field E_x arises behind the laser piston. The electric field grows until it reaches an amplitude sufficient to trap electrons in a potential well formed by both self-consistent plasma and laser ponderomotive force in Figure 5. The adaptation mesh is performed dynamically and controlled by a special criterium. In this work we apply criterium for refinement which analyses the amplitude and first derivative of the local solution trying to keep prescribed resolution. Each newly created cell is initialized in a conservative manner using the cell averages obtained by integration of the reconstruction polynomial over a corresponding control volume. The new electromagnetic Vlasov solver is simple, robust and efficient and can be extended to higher dimensions if needed.

References

[1] K. Kurganov, S. Noelle, G. Petrova, Semi-discrete central-upwind schemes for hyperbolic conservation laws and Hamilton-Jacobi equations, SIAM J. Sci. Comput. 23 (2001) 707–740.

[2] N. V. Elkina, A, An adaptive grid refinement method for the relativistic Vlasov-Maxwell equations., submitted to Journal of Computational Physics.

[3] T. Schlegel, N. Naumova, V. T. Tikhonchuk, C. Labaune, I. V. Sokolov, G. Mourou, Relativistic laser piston model: Ponderomotive ion acceleration in dense plasmas using ultraintense laser pulses, Physics of Plasmas 16 (8) (2009) 083103.